Adipogenic activity of chemicals used in plastic consumer products

Johannes Völker[1*], Felicity Ashcroft[1], Åsa Vedøy[1], Lisa Zimmermann[2] and Martin Wagner[1]

[1] Department of Biology, Norwegian University of Science and Technology (NTNU), 7491 Trondheim, Norway

[2] Department of Aquatic Ecotoxicology, Goethe University Frankfurt am Main, 60438 Frankfurt am Main, Germany

*Johannes Völker

Email: johannes.voelker@ntnu.no

Author Contributions: J.V., F.A. and M.W. conceived the study, J.V. and Å.V. performed the experiments, L.Z. performed the chemical analysis, J.V., F.A., and M.W. analyzed the data and wrote the manuscript, and all authors provided comments on the manuscript.

Keywords: Adipogenesis, endocrine disrupting chemicals, metabolic disruptors, non-target chemical analysis, obesogens

Abstract

Epidemiological studies suggest that obesity cannot solely be attributed to genetics and lifestyle. Accordingly, other environmental factors, such as the exposure to metabolism disrupting chemicals (MDCs), must contribute. Bisphenols or phthalates, prominent chemicals used in plastic, disrupt metabolism and promote obesity in cell and animal models. However, these compounds represent only a very small fraction of plastic chemicals. To investigate whether MDCs are present in plastics, we characterized the adipogenic activity of the chemical mixtures extracted from consumer products covering eight major polymers. We conducted adipogenesis assays with 3T3-L1 cells using high-content fluorescence imaging combined with reporter gene assays for peroxisome proliferator-activated receptor γ (PPARγ) and glucocorticoid receptor (GR), as well as nontarget high-resolution mass spectrometry. Eleven out of 34 plastic products contained chemicals inducing adipogenesis. Polyvinyl chloride (PVC) and polyurethane (PUR), followed by polypropylene (PP), polystyrene (PS), and low-density polyethylene (LDPE) products induced potent adipogenic responses. Compared to rosiglitazone, adipocytes were larger and accumulated more triglycerides in 9 active samples. None of the samples activated GR, and no or a low activation of PPARγ was observed for most adipogenic samples. In total, the products contained 55,300 extractable chemicals, out of which we tentatively identified 2364 unique compounds, including 11 known MDCs. Our results suggest that plastic consumer products contain potent mixtures of MDCs that induce adipogenesis and may promote development to unhealthy adipocytes via PPARγ- and GR-independent mechanisms. Other than well-known MDCs are likely causing these effects.

Introduction

Obesity is a global pandemic that generates a considerable burden of disease, in particular considering comorbidities such as type 2 diabetes, cardiovascular diseases, hypertension, non-alcoholic fatty liver, stroke, and certain types of cancer (1). Worldwide, the number of obese people has nearly tripled since 1975, and more than 41 million children under the age of five were overweight or obese in 2016 (2). This is problematic since a high body mass index (BMI) is one of the top risk factors for deaths (3), and overweight in childhood or adolescence is a good predictor of adult obesity (4). Accordingly, a high BMI contributed to four million deaths globally in 2015 with cardiovascular diseases as leading cause of death followed by diabetes, chronic kidney diseases and cancer (5).

This public health problem has mainly been attributed to genetic background and changes in lifestyle, such as diet, exercise, sleep deficiency, and aging. However, epidemiological evidence suggests that these factors insufficiently explain the magnitude and speed of the obesity pandemic (6). For instance, even when normalizing for caloric intake and exercise, the BMI of US adults increased by 2.3 kg m^{-2} in 2006 compared to 1998 (6). Consequently, identifying and understanding other environmental factors than lifestyle is crucial to manage obesity (7). Given that the endocrine system controls appetite, satiety, metabolism, and weight, exposure to endocrine disrupting chemicals is one such factor (8). In addition to prominent endocrine disruptors, such as the biocide tributyltin and the pesticide dichlorodiphenyltrichloroethane (DDT), plastic chemicals such as bisphenols or phthalates disrupt metabolic functions and promote obesity in cell and animal experiments (8). This is further supported by epidemiological studies that have linked weight gain in humans to bisphenol A (BPA) exposure (9), while contradicting outcomes have been reported regarding a link to phthalate exposure (10-12).

Considering the chemical complexity of plastic consumer products, bisphenols and phthalates represent only the tip of the iceberg. A final article often consists of one or more polymers, multiple intentionally added substances, such as fillers or additives, as well as non-intentionally added

substances, for instance residues from the manufacturing (13). Based on regulatory inventories, over 4000 substances are associated with plastic food packaging alone (13) and, overall, 10,547 chemicals are known to be used in plastics (14). Moreover, empirical data suggests that plastics contain more chemicals than currently known. Using nontarget chemical analysis, we detected hundreds to thousands of chemicals in plastic consumer products, most of these remaining unknown (15). Importantly, the totality of plastic chemicals in a product was toxic *in vitro*, inducing baseline toxicity, oxidative stress, cytotoxicity, and endocrine effects.

Building on these results and the fact that bisphenols and phthalates are known metabolism disrupting chemicals (MDCs; 8, 16, 17), we hypothesized that MDCs are present in plastic consumer products and that metabolic disruption might represent a common but understudied toxicological property of plastic chemicals. To explore this, we used the same plastic consumer products we have extensively characterized previously (15), and investigated the extracts' adipogenic activity in differentiation experiments with murine 3T3-L1 cells. Following exposure to MDCs, 3T3-L1 preadipocyte differentiate into adipocytes, accumulate triglycerides until they finally resemble mature white fat cells (18). The bioassay targets the induction of adipogenesis at the cellular level and represents a well-established *in vitro* model for metabolic disruption *in vivo* (19). We performed optimization experiments and applied high-content fluorescence microscopy combined with an automated image processing to increase the sensitivity and throughput. We also investigated the underlying mechanisms of the adipogenic response and tested whether the extracted plastic chemicals activate the human peroxisome proliferator-activated receptor gamma (PPARγ) or glucocorticoid receptor (GR). We selected PPARγ as a key regulator of adipogenesis (20), and included GR because glucocorticoids are important regulators of lipid metabolism (21). Accordingly, an excess of agonists for these receptors is associated with obesogenic effects in animal models and humans (e.g., weight gain; 19). Moreover, we performed nontarget, ultra-high performance liquid chromatography coupled to a quadrupole of flight spectrometer (LC-QTOF-MS/MS) to characterize the chemicals present in plastics and compare these with a list of compounds known to induce adipogenesis.

Results

Adipogenic activity of plastic consumer products. To exclude cytotoxic effects masking the adipogenic response, we used the nuclei count data to assess cytotoxicity. Most of the extracts were not cytotoxic up to the maximum concentration tested (3 mg plastic well^{-1}), except for PP 4, PUR 3 and PUR 4. The latter two were the most cytotoxic samples with the highest noncytotoxic concentration (HNC) of 0.75 mg plastic well^{-1}. The HNC for PP 4 was 1.5 mg plastic well^{-1} (SI *Appendix*, Fig. S1). To assess the induction of adipogenesis by the plastic extracts, we present the numbers of adipocytes and mature adipocytes in the cell populations and the total lipid droplet count per image for the HNC of each sample. Data were compared to both vehicle and rosiglitazone–treated controls (Fig. 1). Further specifications on the endpoints of the automated image processing, dose-response relationships and example images can be found in the supplementary Information (SI *Appendix*, Fig. S2–S17).

The extracts of eleven plastic consumer products induced adipogenesis with four samples having an equal or stronger effect than the maximal response of cells exposed to rosiglitazone (PVC 2 and 4, PP 4, PUR 3). Similarly to rosiglitazone (Fig. 1A), the proliferative effects induced by plastic extracts were due to an increase in the numbers of adipocytes and mature adipocytes, while the number of preadipocytes remained stable (Fig. 1C). Regarding the polymer type, the most potent extracts were PUR and PVC, with seven out of eight samples inducing adipogenesis, whereas for PP, PS and LDPE only specific samples induced adipogenic responses. In contrast, PET, HDPE, and PLA samples were consistently inactive. The same pattern is reflected by the lipid droplet count data (Fig. 1D). Here, however, some additional samples induced a slight increase in lipid droplets (LDPE 1, PS 1, PP 2).

Given the propensity of environmental pollutants to promote unhealthy adipogenesis, we used the single-cell data to explore a size shift towards hypertrophy and increased accumulation of triglycerides in comparison to rosiglitazone (Fig. 2). We here present the results of one out of four experiments due to the large size of the dataset (results of the other experiments in SI *Appendix*

Fig. S18). Exposure to rosiglitazone dose-dependently increased the lipid content of adipocytes with a median lipid droplet area of 137 pixels $cell^{-1}$ in the lowest concentration to 290 pixels $cell^{-1}$ in the highest concentration (Fig. 2A). The average fluorescence intensity of the lipid droplets remained stable (Fig. 2B), thus the adipocytes increased in size in response to rosiglitazone but triglyceride accumulation within the droplets remained constant. Compared with the maximal response to rosiglitazone, adipocytes exposed to many of the active plastic extracts had a higher lipid content, resulting both from an increase in the size of the adipocytes and from the amount of triglycerides contained within the lipid droplets. The lipid droplet area per adipocyte was greater in nine out of the eleven active samples with a median increase of 21.6–114% (PS 2–LDPE 4). In line with that, the average fluorescence intensity was higher in ten out of the eleven active samples with a median increase of 25.1–60.4% (PS 2–PVC 4). These effects are consistent over all experiments, except for PVC 3 (SI *Appendix* Fig. S18).

Reporter gene assays. We observed a higher cytotoxicity of the extracts on the U2OS cells compared to the 3T3-L1 cells with five samples being cytotoxic. The most cytotoxic sample was PP 4 with a HNC of 0.19 mg plastic $well^{-1}$, followed by PS 2, PP 3 and PLA 1 as well as PVC 2 with a HNC of 0.38 and 0.75 mg plastic $well^{-1}$, respectively (SI *Appendix* Tab. S1).

None of the samples activated GR (SI *Appendix* Fig. S19) and five extracts activated PPARγ (Fig. 3A). PLA1 was the most potent sample with a median receptor activity of 34.7%, followed by PS 2 (24.4%), PVC 2 (10.3%), LDPE 2 (8.4%) and PVC 1 (7.3%). Accordingly, the PPARγ activity of plastic chemicals is a poor predictor of their adipogenic activity (Fig. 3B), except for PVC 2 and PS 2. These two samples induced both PPARγ and adipogenesis at similar effect concentrations. Moreover, three out of the five samples activating PPARγ did not induce adipogenesis in 3T3-L1 cells (PLA 1, LDPE 2, PVC 1).

Chemicals tentatively identified in plastics. Using nontarget GC-QTOF-MS/MS, we previously identified 260 unique chemicals in extracts of the same plastic products (15). This corresponds to 231 tentatively identified chemicals with 227 unique PubChem CIDs in the samples used in this study (SI Appendix Tab. S2). In the nontarget LC-QTOF-MS/MS analysis, we detected in total

55,300 features (i.e., unidentified chemicals) across all samples that were only present in samples or had a >10-fold higher abundance compared to the blanks. Here, the number of features in individual samples ranged from 107 (HDPE 2) to 6242 (PUR 3, Tab. 1). In total, 5500 features had spectral MS/MS data we could use for compound identification, out of which we detected between 30 (PS 4) and 2117 features (PUR 3) per sample.

For tentatively identifying the plastic chemicals, we used the MS/MS data with the MassBank library (14,788 compounds) and three *in silico* fragmented databases of chemicals potentially used in plastics or (pre-)registered for authorization on the European market (in total 75,510 compounds; 22). These queries resulted in a successful identification of 2364 features across all samples, corresponding to 629 unique chemicals (SI *Appendix* Excel Tab. S1). Accordingly, between 6 (PLA 2) and 33 % (PET 1) of the features in each sample were tentatively identified. For the 25 compounds with the highest identification scores (≥ 50) and abundance in the samples, we confirmed the plausibility of the identification by checking whether the compounds are known to be used in plastics (SI *Appendix* Excel Tab. S2). We found that 14 out of 25 compounds are used in plastics, including five plasticizers (e.g., acetyl tributyl citrate), four flame retardants (e.g., tris(2-butoxyethyl) phosphate, tris(3-methylphenyl) phosphate) and multiple processing aids, such as the lubricant 2-nonyl-N-(2-nonylphenyl) aniline, the hardener 4-methylphthalic anhydride and the slip additive (Z)-docos-13-enamide. We also identified compounds that likely migrated from the packed content into the packaging (two octadecanamides used in cosmetics) and one compound that was implausible (the veterinary drug febarbamate).

When cross-referencing the chemicals tentatively identified in plastics and a list of known MDCs inducing adipogenesis in 3T3-L1 cells (SI *Appendix* Tab. S3), we found eleven compounds known to induce adipogenesis *in vitro*. The MDCs present in our samples include four phthalates and six organophosphates (Tab. 1). Benzyl butyl phthalate (BBP), di-butyl phthalate (DBP) and di(2-ethylhexyl) phthalate (DEHP) were present in PVC 4. Di-iso-nonyl phthalate (DINP) was detected in PVC 3 and 4. Diphenyl phosphate (DPP), 2-ethylhexyl diphenyl phosphate (EHDP) and triphenyl phosphate (TPP) were detected in multiple samples. When using raw abundance as a proxy for

concentration, the high levels of TPP, DPP and EHDP (the MDCs present in at least three samples) were detected in two to three active PVC samples (SI *Appendix* Tab. S4). In contrast, the other active samples contain very low levels of these chemicals (PS 2, PP 4, PUR 2, PUR 3). Interestingly, we did not detect organotin compounds or bisphenols (SI *Appendix* Excel Table S1) despite these are known MDCs and thought of as being common in PVC and other plastics (16, 17).

Discussion

Adipogenic activity of plastic consumer products. We hypothesized that plastic products contain MDCs based on the fact that a small set of compounds used in plastics is known to induce adipogenesis *in vitro* and *in vivo* (8, 16, 17). However, the current focus on few, individual plastic chemicals neglects the chemical complexity of plastic materials given that we know that thousands of compounds are either used in plastics or non-intentionally present (13, 14). Thus, we decided to characterize the adipogenic activity of all compounds extractable from plastic consumer products.

Eleven out of 34 products contain chemicals that induce adipogenesis and are, thus, MDCs *in vitro* (Fig. 1). The chemicals extracted from some plastics are not only quite potent but also trigger effects that are similar to or higher than those induced by the reference compound rosiglitazone (PVC 2 and 4, PP 4). Supramaximal efficacies have previously been reported for single compounds, such as dibutyl phthalate and tert-butyl phenyl diphenyl phosphate (23) but only at concentrations ≥10 μM, illustrating the potency of the extracted mixtures.

Products with multiple applications, including two FCMs (PS 2, PP 3) and nine non-FCMs, contain adipogenic chemicals. While chemicals migrating from packaging into food represent an obvious source of human exposure (24), compounds released from non-FCMs can also contribute via dermal uptake (e.g., PUR 4 shower slippers) or inhalation. For instance, dust has been shown to contain chemical mixtures that induce adipogenesis (23). Here, we show that plastic flooring (e.g., PVC 4) contains MDCs that may contribute to human exposure if they partition into dust. Given the

potency of the extracted mixtures and considering our close and constant contact with plastics, it appears plausible that plastic chemicals contribute to an obesogenic environment and, thus, the obesity pandemic.

The chemicals present in PVC and PUR products most consistently induce potent adipogenic responses, while compounds extracted from PET, HDPE, and PLA products were inactive. Apart from PLA samples, this is in line with our previous findings for other toxicity endpoints (15). This suggests that PVC and PUR are more likely to contain MDCs compared to other polymers. However, the chemicals extracted from some PP, PS, and LDPE products also induce adipogenesis (Fig. 1). This supports the idea that caution is needed when trying to generalize the occurrence of toxic chemicals based on polymer type (15).

Unhealthy or dysfunctional adipocytes are part of the obesity phenotype. They are larger in size, have an impaired glucose uptake and insulin signaling, an elevated inflammatory response and decreased respiration (25). While we did not investigate the latter characteristics, adipocytes exposed to plastic chemicals were larger and contained more triglycerides compared to those treated with rosiglitazone (Fig. 2). While rosiglitazone promotes the development of healthy white adipocytes (26, 27), these results suggest that exposure to plastic chemicals could shift adipocytes towards an unhealthy phenotype. Similar trends have been reported for a range of MDCs, including BPA (28) and organotin compounds (29, 30) as well as TPP (31), which we frequently detected in our samples (Tab. 1). Hence, it will be interesting to investigate whether plastic chemicals also trigger the other hallmarks of unhealthy, dysfunctional adipocytes.

Plastic chemicals and adipogenesis. Using nontarget high resolution mass spectrometry, we show that plastic products contain hundreds to thousands of extractable chemicals; few of those identifiable using spectral libraries and *in silico* tools. This is in line with our previous research (15, 22) and points towards the presence of unknown chemicals in plastics (e.g., non-intentionally added substances). Accordingly, the relatively low identification performance in our study is a result of the limited coverage of chemical databases. These limitations notwithstanding, we tentatively

identified a range of known plastic chemicals providing confidence in the accuracy of the identifications.

Plastic products contain known MDCs, including four phthalates (only in PVC 3 and 4) and six organophosphates (Tab. 1). Biomonitoring data suggests that humans are commonly exposed to some of these compounds (32-34). As an example, the phthalates DBP and DEHP as well as the flame retardants TPP and TBEP we found in plastics were recently detected in matched maternal and cord blood samples (35). Accordingly, plastic products can be one source of exposure to these known MDCs.

Known MDCs may explain the adipogenic response to chemicals extracted from some but not all plastic samples. Most active samples contain at least one MDC with TPP, DPP and EHDP being present in multiple samples. Interestingly, the floor covering (PVC 4) contained ten known MDCs. While the active PVC samples contain high levels of TPP, DPP and EHDP, the abundance of these chemicals was very low in the other active samples (SI *Appendix* Tab. S4). This suggests that other than the known MDCs contribute to the adipogenesis induced by plastic chemicals.

Underlying mechanisms. PPARγ is a key regulator of adipogenesis (20), and many MDCs that induce adipogenesis also activate PPARγ (17). Despite the common idea that PPARγ activation is a main mechanism via which anthropogenic chemicals trigger adipogenesis, most of the adipogenic plastic samples in fact do not activate this receptor (Fig. 3). Only in two cases (PVC 2, PS 2) does a high PPARγ activity correspond to a strong induction of lipid droplet formation. Moreover, three samples (PLA 1, LDPE 2, PVC 1) activated PPARγ but were inactive in the adipogenesis assay. Thus, the adipogenic effects of the plastic extracts is not necessarily dependent on direct activation of PPARγ and other mechanisms must be involved.

GR is another important nuclear receptor that participates in adipogenesis, and various MDCs activate GR (36). In particular, glucocorticoids are essential in inducing adipocyte differentiation (SI *Appendix* Fig. S20). However, none of the plastic extracts activated GR rendering this an unlikely mechanism of action in this case.

Elucidating the mechanism by which plastic chemicals induce adipogenesis is complex since we are dealing with two black boxes, namely the complex chemical mixtures present in plastics and the multitude of potential mechanism of actions involved in adipogenic responses in 3T3-L1 cells (19). In addition to PPARγ and GR, (ant)agonists of multiple other nuclear receptors, such as the retinoid x receptor α, estrogen receptor, androgen receptor, liver x receptor, thyroid receptor β, have been demonstrated or are discussed to contribute to an adipogenic response (37). In the light of the diversity of compounds we detected in plastics, it appears probable that these act via multiple mechanisms that are in most cases PPARγ and GR independent. Although more work needs to be done to elucidate the underlying mechanisms, our results underline the importance of using integrative methods, such as the adipogenesis assay to identify MDCs triggering cellular responses rather than assessing (anta)agonism at selected nuclear receptors.

Limitations and future directions. To the best of our knowledge, this is the first study investigating the adipogenic activity of chemicals extractable from plastic consumer products. Considering the diversity of plastic products and their chemical composition, the sample set is certainly not representative of all plastic chemicals, humans will be exposed to. While it is challenging to comprehensively characterize the human exposure to plastic chemicals from all types of products, given their ubiquity and diversity, a way forward is to prioritize polymer types that are likely to contain MDCs, such as PVC and PUR.

Given that our aim was to investigate whether MDCs are present in plastic products, we used methanol to extract the samples. This simulates a worst-case scenario. Thus, even though we demonstrated that potent (mixtures of) MDCs are present in consumer products, it remains to be investigated whether these will migrate under more realistic conditions into air, water or food, or can be taken up dermally. Using the same samples as in the present study, we recently demonstrated that a significant number of chemicals and *in vitro* toxicity, such as antiandrogenic compounds, migrate into water (22). However, it remains unknown if this is also the case for the present MDCs.

Moreover, we analyzed food packaging that contained foodstuff because we aimed at investigating final products. Since chemical migration is not a one-way street, we cannot exclude that compounds present in the packed food migrated into the packaging. The detection of compounds used in cosmetics in packaging underlines this limitation. These compounds may contribute to the observed adipogenic activity or PPARγ activation and future research should cover final FCMs that have not been in contact with food.

The nontarget chemical analysis resulted in the tentative identification of several MDCs. However, many compounds remain unidentified and there is some likelihood of false-positive identifications. The challenge of a rather low identification success is well-known for environmental pollutants (38) and can be addressed by building more comprehensive spectral databases. Recent efforts to build specific databases for plastic chemicals are promising (13, 14) but must be complemented with spectral information and non-intentionally added substances. Moreover, we show that known MDCs only partially – if at all – contribute to the adipogenesis induced by plastic extracts. This points towards the presence of unidentified MDCs in plastics. To identify the compounds that are indeed causative for the observed responses, future research should apply effect-directed analysis. Moreover, our results indicate that plastic chemicals may promote a development towards unhealthy adipocytes. However, more evidence is needed to further support this hypothesis. For instance, one needs to extend the adipogenesis assay to cover later stages of adipocyte development and investigate biomarkers of inflammation and metabolic function (e.g., glucose uptake, insulin sensitivity).

Taken together, we demonstrated that plastic consumer products contain potent (mixtures of) MDCs inducing adipogenesis *in vitro* via mechanisms that are mostly not mediated via PPARγ and GR. Accordingly, plastic chemicals may contribute to an obesogenic environment considering our constant contact with a broad range of plastic products. Given that the plastic products containing MDCs also contained compounds triggering other toxicological endpoints (15), a shift towards chemically less complex plastics represents a way forward to a non-toxic environment.

Materials and Methods

A list of used chemicals is provided in SI *Appendix* (Tab. S5).

Sample selection and plastic extraction. We used the same 34 plastic samples (Tab. 1) as in Zimmermann *et al.* (15). The samples cover petroleum-based polymers with the highest market share (polypropylene (PP) > low density polyethylene (LDPE) > high density polyethylene (HDPE) > polyvinyl chloride (PVC) > polyurethane (PUR) > polyethylene terephthalate (PET) > polystyrene (PS); 39), and polylactic acid (PLA) as a bio-based alternative. The samples include 21 products with and 13 products without food contact. Further specifications on the sample selection, collection and polymer identification are described in Zimmermann *et al.* (15). We extracted 3 g sample with including three procedure blanks (PB 1-3) with methanol and concentrated the extracts to a final volume of 200 µL using dimethyl sulfoxide as a keeper. To contextualize the bioassay results, we use "plastic equivalents" in such that "1 mg plastic" corresponds to the chemicals extracted from 1 mg of plastic. Accordingly, 1 µl extract corresponds to 15 mg plastic. See SI *Appendix* for details.

Bioassays. We performed differentiation assays with murine 3T3-L1 adipocytes (Zenbio Inc., SP-L1-F, lot 3T3L1062104) to examine the induction of adipogenesis as well as CALUX reporter gene assays (BioDetection Systems B.V., Amsterdam, The Netherlands) to investigate the agonistic activity at the human peroxisome proliferator-activated receptor γ (40) and glucocorticoid receptor (GR, 41). All experiments were conducted with negative controls, vehicle controls, positive controls, and PB 1–3. Samples, controls, and blanks were diluted 1000-fold (adipogenesis assay) or 500-fold (reporter gene assays) with medium, resulting in a maximum final solvent concentration of 0.1% or 0.2% (v/v), respectively. Each sample was analyzed in serial dilutions of 1:2 with four replicates per concentration in at least three independent experiments per assay. Moreover, the respective reference compound was included on every microtiter plate to control for potential variations between plates, and the sample arrangement was randomized to exclude position effects. As negative and vehicle controls did not differ significantly, the results from both were

pooled. Further, there was no contamination during sample extraction and analysis since none of the controls and blanks induced activity (SI *Appendix* Fig. S21 and S22). See SI *Appendix* for details on the cell culture conditions.

Adipogenesis assay. We performed the differentiation assay with 3T3-L1 cells in accordance with a previously described method (42). In brief, an experiment consists of three days pre-differentiation (one day seeding, two days allowing cells to enter the resting state) followed by an 8-d differentiation window (two days differentiation, six days maintenance). Subconfluent cells of passage 10 were trypsinized and counted with a flow cytometer (NovoCyte, Acea Biosciences). 15,000 cells well^{-1} were seeded in 200 µL preadipocyte medium (PAM: DMEM-high supplemented with 10% bovine calf serum and 1% penicillin/streptomycin) into 96-well black, clear bottom tissue culture plates (655090, Greiner Bio-One) and incubated at 37 ℃ and 5% CO_2. After 24 h, we checked that the cells reached confluency, replaced the medium with 200 µL fresh PAM well^{-1}, and cultured the cells for another 48 h to initiate growth arrest. We included on every plate a pre-adipocyte control (undifferentiated cells) which was kept in PAM, while the rest of the cells were differentiate as described below.

Optimization experiments. Given that a systematic analysis of dexamethasone (DEX) effects on triglyceride accumulation and differentiation efficiency in 3T3-L1 cells was lacking, we conducted optimization experiments to identify a suitable DEX concentration to initiate adipocyte differentiation that results in the lowest baseline as well as the highest sensitivity and dynamic range when co-exposed to the reference compound rosiglitazone. Moreover, we compared two methods to quantify triglycerides based on Nile Red Staining. We determined the total NileRed fluorescence well^{-1} and compared it to an automated imaging and analysis platform to determine whether the latter improves the sensitivity and dynamic range for the screening of adipogenic activity.

Based on the results (SI *Appendix* Figure S20) and in comparison with previous studies, we found that a rather low optimal DEX concentration (6.25 nM) was sufficient to initiate adipocyte differentiation without increasing the assay's baseline. Compared to the fluorescence readout well-

[1], an automated imaging approach is more sensitive to assess proliferation, enhances the dynamic range of the assay (SI *Appendix* Fig. S20) and provides more information because it enables single-cell analysis for a more in-depth characterization of the adipocyte population (pre-adipocytes, adipocytes and mature adipocytes). Accordingly, we analyzed the effects of the plastic extracts using 6.25 nM DEX during the differentiation window and the automated imaging approach. See SI *Appendix* for details.

Dosing of samples. To initiate differentiation, we replaced the PAM medium with 200 µL differentiation medium well^{-1} (DM: DMEM-high supplemented with 10% FBS, 1% penicillin/streptomycin, 20 mM HEPES, 1 µg mL^{-1} insulin, 0.5 mM 3-isobutyl-1-methylxanthine (IBMX), and 6.25 nM DEX) containing 5 concentrations of samples serially diluted 1:2 (0.19–3 mg plastic well^{-1} equivalent to 0.94–15 mg plastic mL^{-1}) or rosiglitazone (1.17–300 nM). Following the 48-h differentiation, the medium was replaced with 200 µL adipocyte maintenance medium well^{-1} (DM without IBMX and DEX) containing the respective controls, samples, or rosiglitazone and changed the medium every other day during the 6d maintenance period.

Fixation and staining. After 11 d, cells were fixed with 2% paraformaldehyde and co-stained with NileRed and NucBlue. Imaging was carried out on the Cytation 5 Cell Imaging Multimode reader (BioTek). Three images per field (Brightfield, NucBlue and NileRed) and nine fields per well were captured. See SI *Appendix* for details.

Image analysis. Images were analyzed in the open-source software CellProfiler (43). A description of the image analysis protocol and the CellProfiler pipelines are available in the SI *Appendix*. We quantified proliferation (nuclei count), number of lipid droplets (lipid droplet count), total area occupied by lipid droplets (total area), and the total intensity of the NileRed staining within the lipid droplets (total intensity) per image. We further quantified the total area occupied by lipid (lipid droplet area), and the total intensity of NileRed staining in the lipid droplet area per cell. Analysis of the single-cell data was applied to quantify the numbers of adipocytes and mature adipocytes

per image. An adipocyte was defined as a cell containing at least one lipid droplet and a mature adipocyte was defined as a cell containing a total lipid content equivalent to ≥ 8 average sized lipid droplets (1000 pixels).

Single-cell measurements of lipid droplet area, and NileRed staining were analyzed further to explore how triglyceride accumulation was distributed within an adipocyte population. To control for potential cross-plate differences in staining intensity within an experiment, the average fluorescence intensity per adipocyte was normalized to the mean average fluorescence intensity for an internal plate control (cells treated with 300 nM rosiglitazone). For an independent experiment, single-cell data were grouped based on the treatment. The median lipid droplet area and normalized average fluorescence intensities per cell were calculated for each experiment. An example of the images and visualized output of the image analysis is shown in SI *Appendix* (Fig. S2).

Reporter gene assays. We performed the CALUX reporter gene assays in 384-well plates and used imaging to count nuclei per well to normalize the reporter gene response and assess cytotoxicity. Rosiglitazone was the reference compound for PPARγ and DEX for GR (SI *Appendix* Fig. S23). See SI *Appendix* for the detailed protocol.

Analysis of bioassay data. We used GraphPad Prism 9 (GraphPad Software, San Diego, CA) for non-linear regressions and statistical analysis, and interpolated plastic equivalents inducing 10 or 20% effect (effect concentration, EC_{10} or EC_{20}) from the respective dose-response curves. The limit of detection (LOD) of each endpoint and experiment was calculated as three times the standard deviation (SD) of pooled controls. See SI *Appendix* for details.

Nontarget chemical analysis. We analyzed all samples, except PLA 3, using ultra-high performance liquid chromatography coupled to a quadrupole time of flight spectrometer (LC-QTOF-MS/MS) with an Acquity UPLC Waters liquid chromatography system coupled to a SYNAPT G2-S mass spectrometer (both Waters Norge, Oslo, Norway). The analytical method has been described

in Zimmermann *et al.* (22, 44) and a brief description as well as information about the data analysis and compound identification can be found in SI *Appendix*.

Comparison with chemicals known to induce adipogenesis. We built a list of 120 know adipogenic chemicals (SI *Appendix* Tab. S3) by searching Web of Science (Core Collection) for studies investigating chemicals in the adipogenesis assay and complemented the search with chemicals reviewed by Amato *et al.* (16). We cross-referenced the list with the tentatively identified compounds in the plastic samples to determine whether some of these compounds are MDCs (Tab. 1). See SI *Appendix* for details.

Data Availability

The raw mass spectral data can be accessed under DOI 10.5281/zenodo.4781257 (published after publication), bioassay data (SI *Appendix* Excel Tab. S3–10) and the CellProfiler pipelines can be found in SI *Appendix*.

Acknowledgments

This study was support by internal funding of the Norwegian University of Science and Technology (NTNU, Trondheim). We thank Susana Villa Gonzales (NTNU) for UPLC-QTOF-MS/MS training and support.

References

1. Swinburn BA, Kraak VI, Allender S, Atkins VJ, Baker PI, Bogard JR, et al. The global syndemic of obesity, undernutrition, and climate change: The Lancet Commission report. Lancet. 2019; 393: 791-846.
2. WHO (2018). Obesity and overweight. Fact sheet, World Health Organization, Geneva, Switzerland. [cited 2021 July 28] Available at: https://www.who.int/news-room/fact-sheets/detail/obesity-and-overweight
3. Gakidou E, Afshin A, Abajobir AA, Abate KH, Abbafati C, Abbas KM et al. Global, regional, and national comparative risk assessment of 84 behavioural, environmental and occupational, and metabolic risks or clusters of risks, 1990-2016: a systematic analysis for the Global Burden of Disease Study 2016. Lancet. 2017; 390: 1345-422.
4. Simmonds M, Llewellyn A, Owen CG, Woolacott N. Predicting adult obesity from childhood obesity: a systematic review and meta-analysis. Obes Rev. 2016;17: 95-107.
5. Afshin A, Forouzanfar MH, Reitsma MB, Sur P, Estep K, Lee A, et al. Health Effects of Overweight and Obesity in 195 Countries over 25 Years. N Engl J Med. 2017; 377: 13-27.
6. Brown RE, Sharma AM, Ardern CI, Mirdamadi P, Mirdamadi P, Kuk JL. Secular differences in the association between caloric intake, macronutrient intake, and physical activity with obesity. Obes Res Clin Pract. 2016; 10: 243-55.
7. Franks PW, McCarthy MI. Exposing the exposures responsible for type 2 diabetes and obesity. Science. 2016; 354: 69-73.
8. Heindel JJ, Blumberg B, Cave M, Machtinger R, Mantovani A, Mendez MA, et al. Metabolism disrupting chemicals and metabolic disorders. Reprod Toxicol. 2017; 68: 3-33.
9. Hoepner LA, Whyatt RM, Widen EM, Hassoun A, Oberfield SE, Mueller NT, et al. bisphenol A and adiposity in an inner-city birth cohort. Environ Health Perspect. 2016; 124: 1644-50.
10. Trasande L, Attina TM, Sathyanarayana S, Spanier AJ, Blustein J. Race/ethnicity-specific associations of urinary phthalates with childhood body mass in a nationally representative sample. Environ Health Perspect. 2013; 121: 501-6.
11. Valvi D, Casas M, Romaguera D, Monfort N, Ventura R, Martinez D, et al. Prenatal phthalate exposure and childhood growth and blood pressure: Evidence from the spanish inma-sabadell birth cohort study. Environ Health Perspect. 2015; 123:1022-9.
12. Buckley JP, Engel SM, Mendez MA, Richardson DB, Daniels JL, Calafat AM, et al. Prenatal phthalate exposures and childhood fat mass in a New York city cohort. Environ Health Perspect. 2016; 124: 507-13.
13. Groh KJ, Backhaus T, Carney-Almroth B, Geueke B, Inostroza PA, Lennquist A, et al. Overview of known plastic packaging-associated chemicals and their hazards. Sci Total Environ. 2019; 651: 3253-68.
14. Wiesinger H, Wang Z, Hellweg S. Deep dive into plastic monomers, additives, and processing aids. Environ Sci Technol. 2021; 55: 9339-51.
15. Zimmermann L, Dierkes G, Ternes TA, Volker C, Wagner M. Benchmarking the in vitro toxicity and chemical composition of plastic consumer products. Environ Sci Technol. 2019; 53:11467-77.

16. Amato AA, Wheeler HB, Blumberg B. Obesity and endocrine-disrupting chemicals. Endocr Connect. 2021; 10: R87-R105.

17. Egusquiza RJ, Blumberg B. Environmental obesogens and their impact on susceptibility to obesity: New mechanisms and chemicals. Endocrinology. 2020; 161: 1-14.

18. Green H, Meuth M. An established pre-adipose cell line and its differentiation in culture. Cell. 1974; 3: 127-33.

19. Kassotis CD, Stapleton HM. Endocrine-mediated mechanisms of metabolic disruption and new approaches to examine the public health threat. Front Endocrinol. 2019; 10: 39.

20. Rosen ED, MacDougald OA. Adipocyte differentiation from the inside out. Nat Rev Mol Cell Biol. 2006; 7: 885-96.

21. John K, Marino JS, Sanchez ER, Hinds TD, Jr. The glucocorticoid receptor: cause of or cure for obesity? Am J Physiol Endocrinol Metab. 2016; 310: E249-57.

22. Zimmermann L, Bartosova Z, Braun K, Oehlmann J, Völker C, Wagner M. Plastic products leach chemicals that induce in vitro toxicity under realistic use conditions. Environ Sci Technol. 2021. Available at: https://doi.org/10.1021/acs.est.1c01103 (in press)

23. Kassotis CD, Hoffman K, Stapleton HM. Characterization of adipogenic activity of house dust extracts and semi-volatile indoor contaminants in 3T3-L1 Cells. Environ Sci Technol. 2017; 51: 8735-45.

24. Muncke J, Backhaus T, Geueke B, Maffini MV, Martin OV, Myers JP, et al. Scientific challenges in the risk assessment of food contact materials. Environ Health Perspect. 2017; 125: 095001.

25. Ghaben AL, Scherer PE. Adipogenesis and metabolic health. Nat Rev Mol Cell Biol. 2019; 20: 242-58.

26. Sharma AM, Staels B. Review: Peroxisome proliferator-activated receptor gamma and adipose tissue--understanding obesity-related changes in regulation of lipid and glucose metabolism. J Clin Endocrinol Metab. 2007; 92: 386-95.

27. Kusminski CM, Bickel PE, Scherer PE. Targeting adipose tissue in the treatment of obesity-associated diabetes. Nat Rev Drug Discov. 2016; 15: 639-60.

28. Ariemma F, D'Esposito V, Liguoro D, Oriente F, Cabaro S, Liotti A, et al. Low-dose bisphenol-a impairs adipogenesis and generates dysfunctional 3T3-L1 adipocytes. Plos One. 2016; 11: e0150762.

29. Regnier SM, El-Hashani E, Kamau W, Zhang X, Massad NL, Sargis RM. Tributyltin differentially promotes development of a phenotypically distinct adipocyte. Obesity. 2015; 23:1864-71.

30. Shoucri BM, Hung VT, Chamorro-Garcia R, Shioda T, Blumberg B. Retinoid x receptor activation during adipogenesis of female mesenchymal stem cells programs a dysfunctional adipocyte. Endocrinology. 2018; 159: 2863-83.

31. Cano-Sancho G, Smith A, La Merrill MA. Triphenyl phosphate enhances adipogenic differentiation, glucose uptake and lipolysis via endocrine and noradrenergic mechanisms. Toxicol In Vitro. 2017; 40: 280-8.

32. Ospina M, Jayatilaka NK, Wong LY, Restrepo P, Calafat AM. Exposure to organophosphate flame retardant chemicals in the U.S. general population: Data from the 2013-2014 national health and nutrition examination survey. Environ Int. 2018; 110: 32-41.

33. Zota AR, Phillips CA, Mitro SD. Recent fast food consumption and bisphenol a and phthalates exposures among the U.S. population in NHANES, 2003-2010. Environ Health Perspect. 2016; 124: 1521-8.

34. Zota AR, Calafat AM, Woodruff TJ. Temporal trends in phthalate exposures: findings from the national health and nutrition examination survey, 2001-2010. Environ Health Perspect. 2014; 122: 235-41.

35. Wang A, Abrahamsson DP, Jiang T, Wang M, Morello-Frosch R, Park JS, et al. Suspect screening, prioritization, and confirmation of environmental chemicals in maternal-newborn pairs from San Francisco. Environ Sci Technol. 2021; 55: 5037-49.

36. Sargis RM, Johnson DN, Choudhury RA, Brady MJ. Environmental endocrine disruptors promote adipogenesis in the 3T3-L1 cell line through glucocorticoid receptor activation. Obesity. 2010; 18: 1283-8.

37. Fu M, Sun T, Bookout AL, Downes M, Yu RT, Evans RM, et al. A nuclear receptor atlas: 3T3-L1 adipogenesis. Mol Endocrinol. 2005; 19: 2437-50.

38. Hollender J, Schymanski EL, Singer HP, Ferguson PL. Nontarget screening with high resolution mass spectrometry in the environment: Ready to go? Environ Sci Technol. 2017; 51: 11505-12.

39. Plastic Europe (2020). Plastics–The Facts 2020: An analysis of european plastics production, demand and waste data. [cited 2021 July 28] Available at: https://www.plasticseurope.org/en/resources/publications/4312-plastics-facts-2020

40. Gijsbers L, Man HY, Kloet SK, de Haan LH, Keijer J, Rietjens IM, et al. Stable reporter cell lines for peroxisome proliferator-activated receptor gamma (PPARgamma)-mediated modulation of gene expression. Anal Biochem. 2011; 414: 77-83.

41. Sonneveld E, Jansen HJ, Riteco JA, Brouwer A, van der Burg B. Development of androgen- and estrogen-responsive bioassays, members of a panel of human cell line-based highly selective steroid-responsive bioassays. Toxicol Sci. 2005; 83: 136-48.

42. Kassotis CD, Masse L, Kim S, Schlezinger JJ, Webster TF, Stapleton HM. Characterization of adipogenic chemicals in three different cell culture systems: Implications for reproducibility based on cell source and handling. Sci Rep. 2017; 7: 42104.

43. Carpenter AE, Jones TR, Lamprecht MR, Clarke C, Kang IH, Friman O, et al. CellProfiler: image analysis software for identifying and quantifying cell phenotypes. Genome Biol. 2006; 7: R100.

44. Zimmermann L, Dombrowski A, Völker C, Wagner M. Are bioplastics and plant-based materials safer than conventional plastics? In vitro toxicity and chemical composition. Environ Int. 2020; 145: 106066.

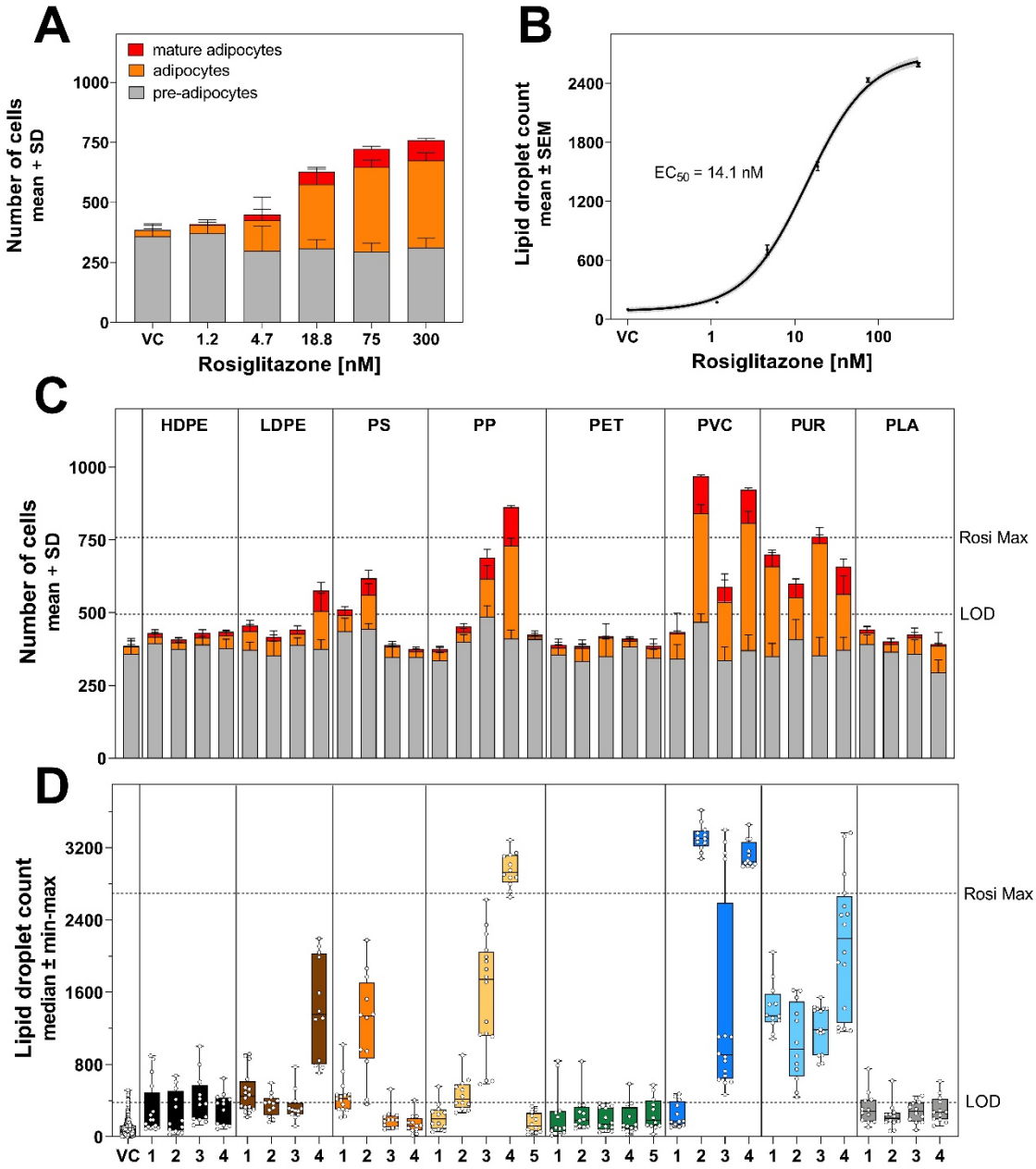

Figure 1. **Effect of rosiglitazone on (A) the adipocyte population and (B) the lipid droplet count (pooled data from four experiments).** Effect of plastic extracts on (C) the adipocyte population and (D) the lipid droplet count in the highest noncytotoxic concentration. The highest noncytotoxic concentration (HNC) was 3 mg plastics well^{-1} except for PP 4 (1.5 mg plastic well^{-1}) as well as PUR 2 and PUR 3 (0.75 mg plastic well^{-1}). VC = vehicle control, LOD = limit of the detection, Rosi Max = maximal response of rosiglitazone.

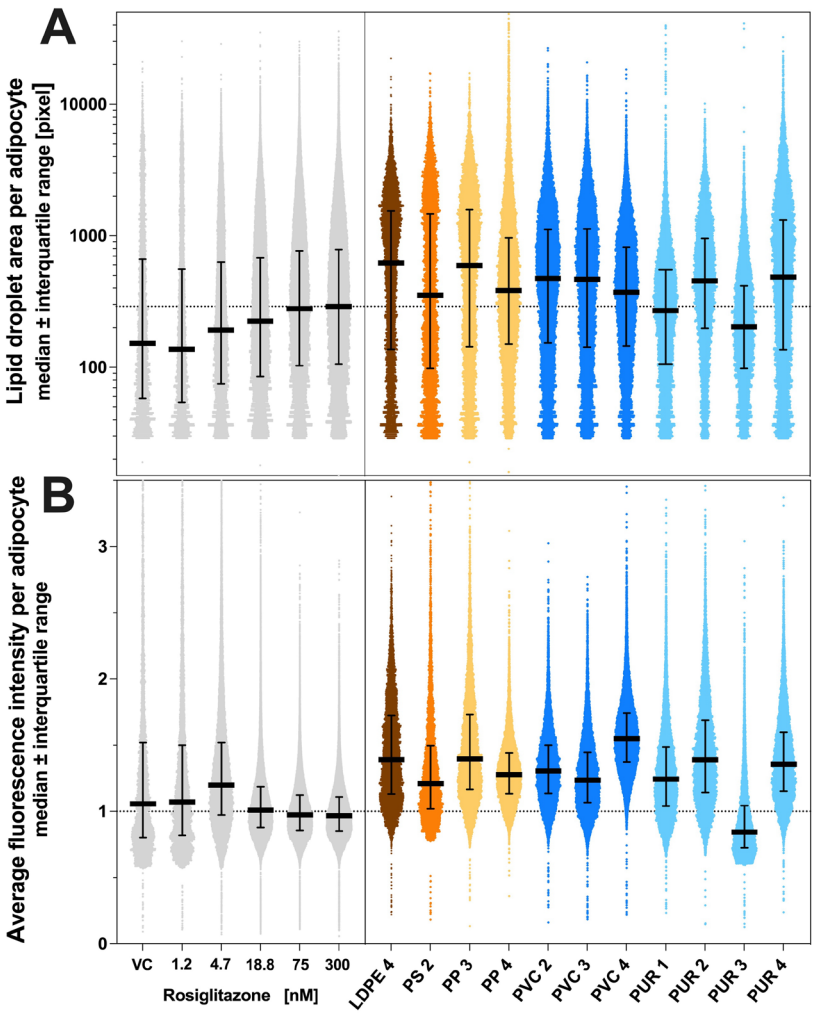

Figure 2. **(A) Size distribution of adipocyte population and (B) accumulation of triglyceride per adipocyte in cells exposed to rosiglitazone (left) or the highest noncytotoxic concentration of the eleven active plastic extracts (right).** Single-cell data from one experiment. Intensity data is normalized on the mean of the highest rosiglitazone concentration (300 nM). VC = vehicle control.

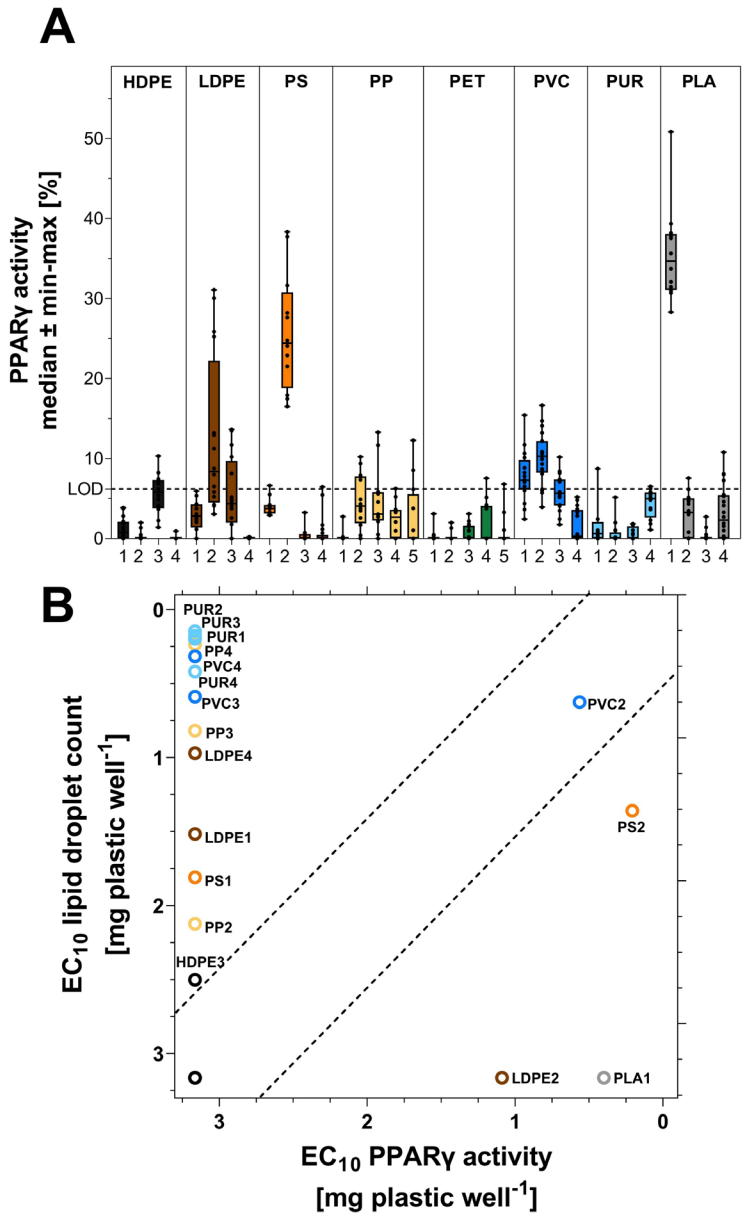

Figure 3. **(A) PPARγ activity induced by plastic extracts at the highest noncytotoxic concentration and (B) correlation of the EC_{10} of the PPARγ activity and lipid droplet count**. The highest noncytotoxic concentration (HCN) was 1.5 mg plastic well^{-1} except for PP 4 (0.19 mg plastic well^{-1}), PS 2 and PP 3 (0.38 mg plastic well^{-1}) as well as PLA 1 and PVC 2 (0.75 mg plastic well^{-1}).

Table 1. Plastic products analyzed in this study, results of the nontarget chemical analysis and the tentatively identified metabolic disrupting chemicals (MDCs).

Sample	Plastic product	LC-QTOF-MS/MS (number of features)					Tentatively identified MDCs
		before filter	≥10-fold vs. blank	with MS2	ID with score ≥40	% of MS2	
HDPE 1	refillable drinking bottle[a]	4488	779	203	38	18.7	TPP
HDPE 2	yogurt drinking bottle[a]	3845	107	34	7	20.6	
HDPE 3	bin liner	5293	614	153	30	19.6	TPP
HDPE 4	shower gel bottle	4290	164	50	16	32.0	EHDP
LDPE 1	lemon juice bottle[a]	4294	241	66	20	30.3	EHDP
LDPE 2	plastic wrap[a]	6596	1833	543	98	18.0	TPP
LDPE 3	freezer bag[a]	6095	1603	416	62	14.9	TPP
LDPE 4	hair conditioner bottle	6653	1702	544	89	16.4	allethrin, TPP
PS 1	yogurt cup[a]	4259	447	96	12	12.5	TPP
PS 2	fruit tray[a]	6097	1122	293	44	15.0	DPP, TPP
PS 3	vegetable tray[a]	4719	308	63	11	17.5	
PS 4	plastic cup[a]	4175	119	30	7	23.3	
PP 1	refillable drinking bottle[a]	8146	1365	396	87	22.0	TPP
PP 2	yogurt cup[a]	7462	1870	549	93	16.9	TPP
PP 3	gummy candy packaging[a]	6671	3159	910	117	12.9	TPP
PP 4	handkerchief packaging	6441	1798	519	85	16.4	TPP
PP 5	shampoo bottle	4240	268	101	29	28.7	
PET 1	soft drink bottle[a]	4261	148	55	18	32.7	
PET 2	yogurt cup[a]	4259	179	51	12	23.5	
PET 3	oven bag[a]	4933	647	159	30	18.9	
PET 4	vegetable tray[a]	5470	695	182	20	11.0	
PET 5	shampoo bottle	5116	375	89	11	12.4	
PVC 1	plastic wrap[a]	8597	3655	1374	118	8.6	
PVC 2	place mat	7974	2426	819	145	17.7	DPP, TPP
PVC 3	pond liner	5987	1270	450	91	20.2	DINP, TPP
PVC 4	floor covering	5313	2361	868	145	16.7	BBP, BPDP, DBP, DEHP, DINP, DPP, EHDP, TBEP, TOCP, TPP
PUR 1	scouring pad	13,251	5619	1773	216	12.2	EHDP, TPP
PUR 2	kids bath sponge	11,020	4521	1182	151	12.8	
PUR 3	acoustic foam	13,375	6242	2117	224	10.6	EHDP, TPP
PUR 4	shower slippers	6142	1035	300	78	26.0	EHDP, TPP
PLA 1	yogurt cup[a]	7172	2421	772	52	6.7	TPP
PLA 2	vegetable tray[a]	6631	1983	672	40	6.0	
PLA 3	coffee cup lid[a]	N/A	N/A	N/A	N/A	N/A	
PLA 4	coffee cup lid[a]	8012	2575	857	73	8.5	

[a] = food contact material, BBP = benzyl butyl phthalate, BPDP = tert-butylphenyl diphenyl phosphate, DBP = dibutyl phthalate, DEHP = bis(2-ethylhexyl) phthalate, DINP = di-iso-nonyl phthalate, DPP = diphenyl phosphate, EHDP = 2-ethylhexyl diphenyl phosphate, N/A = not analyzed, TBEP = tris(2 butoxyethyl) phosphate, TOCP = tri-o-cresyl phosphate, TPP = triphenyl phosphate

Fig. S1. Nuclei count of the cytotoxic plastic extracts (PP 4, PUR 2, PUR 3) in the adipogenesis assay. Data is presented as mean count per field (red lines) from three to four independent experiments performed with four replicates each (dots, n ≥ 12). VC = vehicle control.

Fig. S2. Image analysis example. Differentiated 3T3-L1 cells exposed to rosiglitazone (4.69 nM). (A) Merged brightfield and fluorescence images. Nuclei are stained with NucBlue (blue) and lipid with NileRed (red). (B) Corresponding object identification performed with CellProfiler. Nuclei are outlined in blue, cell boundaries in green, and adipocytes in red. Identified lipid droplets are shown as a solid color and all lipid droplets associated with a given adipocyte are displayed in the same color.

Fig. S3. Dose-response relationship for the reference compound rosiglitazone in the adipogenesis assay with 6.25 nM dexamethasone in the differentiation medium. (A) proliferation normalized on the mean of the vehicle control, (B) lipid droplet count per field, (C) adipocyte count per field, (D) mature adipocyte count per field, (E) total intensity of the NileRed staining within the lipid droplet mask per field and (F) total area occupied by lipid droplets per field. 160 or more replicates per concentration (n ≥ 160). VC = vehicle control, LOD = limit of detection, RFU = relative fluorescence unit.

Fig. S4. Dose-dependent induction of adipogenesis in 3T3-L1 cells exposed to the reference compound rosiglitazone. Merged brightfield and fluorescence images. Nuclei are stained with NucBlue (blue) and triglycerides with NileRed (red). VC = vehicle control. Raw pictures were processed in the same manner for visualization.

Fig. S5. Dose-response relationship for the HDPE plastic extracts (HDPE 1–4) in the adipogenesis assay. (A) proliferation normalized on the mean of the vehicle control, (B) lipid droplet count per field, (C) adipocyte count per field, (D) mature adipocyte count per field, (E) total intensity of the NileRed staining within the lipid droplet mask per field and (F) total area occupied by lipid droplets per field. Twelve or more replicates per concentration (n ≥ 12). LOD = limit of detection, RFU = relative fluorescence unit.

Fig. S6. Dose-response relationship for the LDPE plastic extracts (LDPE 1–4) in the adipogenesis assay. (A) proliferation normalized on the mean of the vehicle control, (B) lipid droplet count per field, (C) adipocyte count per field, (D) mature adipocyte count per field, (E) total intensity of the NileRed staining within the lipid droplet mask per field and (F) total area occupied by lipid droplets per field. Twelve or more replicates per concentration (n ≥ 12). LOD = limit of detection, Max Rosi = rosiglitazone maximal response, RFU = relative fluorescence unit.

Fig. S7. Dose-dependent induction of adipogenesis in 3T3-L1 cells exposed to the active plastic extract LDPE 4. Merged brightfield and fluorescence images. Nuclei are stained with NucBlue (blue) and triglycerides with NileRed (red). Raw pictures were processed in the same manner for visualization.

Fig. S8. Dose-response relationships for the PS plastic extracts (PS 1–4) in the adipogenesis assay. (A) proliferation normalized on the mean of the vehicle control, (B) lipid droplet count per field, (C) adipocyte count per field, (D) mature adipocyte count per field, (E) total intensity of the NileRed staining within the lipid droplet mask per field and (F) total area occupied by lipid droplets

per field. Twelve or more replicates per concentration (n ≥ 12). LOD = limit of detection, RFU = relative fluorescence unit.

Fig. S9. Dose-dependent induction of adipogenesis in 3T3-L1 cells exposed to the active plastic extract PS 2. Merged brightfield and fluorescence images. Nuclei are stained with NucBlue (blue) and triglycerides with NileRed (red). Raw pictures were processed in the same manner for visualization.

Fig. S10. Dose-response relationship for the PP plastic extracts (PP 1–5) in the adipogenesis assay. (A) proliferation normalized on the mean of the vehicle control, (B) lipid droplet count per field, (C) adipocyte count per field, (D) mature adipocyte count per field, (E) total intensity of the NileRed staining within the lipid droplet mask per field and (F) total area occupied by lipid droplets per field. Twelve or more replicates per concentration (n ≥ 12). LOD = limit of detection, Max Rosi = rosiglitazone maximal response, RFU = relative fluorescence unit.

Fig. S11. Dose-dependent induction of adipogenesis in 3T3-L1 cells exposed to the active plastic extracts PP 3 and PP 4. Merged brightfield and fluorescence images. Nuclei are stained with NucBlue (blue) and triglycerides with NileRed (red). Raw pictures were processed in the same manner for visualization.

Fig. S12. Dose-response relationship for the PET plastic extracts (PET 1–5) in the adipogenesis assay. (A) proliferation normalized on the mean of the vehicle control, (B) lipid droplet count per field, (C) adipocyte count per field, (D) mature adipocyte count per field, (E) total intensity of the NileRed staining within the lipid droplet mask per field and (F) total area occupied by lipid droplets per field. Twelve or more replicates per concentration (n ≥ 12). LOD = limit of detection, RFU = relative fluorescence unit.

Fig. S13. Dose-response relationship for the PVC plastic extracts (PVC 1–4) in the adipogenesis assay. (A) proliferation normalized on the mean of the vehicle control, (B) lipid droplet count per field, (C) adipocyte count per field, (D) mature adipocyte count per field, (E) total intensity of the NileRed staining within the lipid droplet mask per field and (F) total area occupied by lipid droplets per field. Twelve or more replicates per concentration (n ≥ 12). LOD = limit of detection, Max Rosi = rosiglitazone maximal response RFU = relative fluorescence unit.

Fig. S14. Dose-dependent induction of adipogenesis in 3T3-L1 cells exposed to the active plastic extracts PVC 2– 4. Merged brightfield and fluorescence images. Nuclei are stained with NucBlue (blue) and triglycerides with NileRed (red). Raw pictures were processed in the same manner for visualization.

Fig. S15. Dose-response relationship for the PUR plastic extracts (PUR 1–4) in the adipogenesis assay. (A) proliferation normalized on the mean of the vehicle control, (B) lipid droplet count per field, (C) adipocyte count per field, (D) mature adipocyte count per field, (E) total intensity of the NileRed staining within the lipid droplet mask per field and (F) total area occupied by lipid droplets per field. Twelve or more replicates per concentration (n ≥ 12). LOD = limit of detection, Max Rosi = rosiglitazone maximal response, RFU = relative fluorescence unit.

Fig. S16. Dose-dependent induction of adipogenesis in 3T3-L1 cells exposed to the active plastic extracts PUR 1-4. Merged brightfield and fluorescence images. Nuclei are stained with

NucBlue (blue) and triglycerides with NileRed (red). Raw pictures were processed in the same manner for visualization.

Fig. S17. Dose-response relationship for the PLA plastic extracts (PLA 1–4) in the adipogenesis assay. (A) proliferation normalized on the mean of the vehicle control, (B) lipid droplet count per field, (C) adipocyte count per field, (D) mature adipocyte count per field, (E) total intensity of the NileRed staining within the lipid droplet mask per field and (F) total area occupied by lipid droplets per field. Twelve or more replicates per concentration (n ≥ 12). LOD = limit of detection, Max Rosi = rosiglitazone maximal response, RFU = relative fluorescence unit.

Fig. S18. Size distribution of adipocyte population (left) and accumulation of triglyceride per adipocyte in cells exposed to rosiglitazone or the highest noncytotoxic concentration of the eleven active plastic extracts. Single-cell data from 4 independent experiments. Intensity data is normalized to the mean of the highest rosiglitazone concentration (300 nM). VC = vehicle control.

Fig. S19. GR activity of plastic extracts at the highest noncytotoxic concentration. Highest noncytotoxic concentration was 1.5 mg plastic well^{-1} except for PP 4 (0.19 mg plastic well^{-1}), PS 2 and PP 3 (0.38 mg plastic well^{-1}), PLA 1, PVC 2 and PVC 4 (0.75 mg plastic well^{-1}). GR = glucocorticoid receptor, LOD = limit of detection. n ≥ 12.

Fig. S20. Optimization of the adipogenesis assay. (A) Proliferative effects induced by rosiglitazone analyzed by imaging (DAPI filter) and total fluorescence readout (NucBlue) with 25 nM dexamethasone (DEX) in the differentiation medium (DM). (B) Multiple adipogenic endpoints analyzed by imaging (RFP filter) compared to total fluorescence readout (NileRed) with 25 nM DEX in DM. (C) Total fluorescence readout (NileRed) for the preadipocyte control (preA, undifferentiated) and the differentiated vehicle controls with increasing dexamethasone concentrations in DM. (D) Lipid droplet count induction by rosiglitazone with 6.25, 12.5, 25 nM DEX in DM.

Fig. S21. Dose-response relationships for the adipogenesis assay endpoints of the three procedure blanks (PB 1–3). (A) proliferation normalized on the mean of the vehicle control, (B) lipid droplet count per field, (C) adipocyte count per field, (D) mature adipocyte count per field, (E) total intensity of the NileRed staining within the lipid droplet mask per field and (F) total area occupied by lipid droplets per field. Twelve replicates per concentration (n = 12). LOD = limit of detection, RFU = relative fluorescence unit.

Fig. S22. Dose-response relationships for (A) PPARγ and (B) GR activity of the three procedure blanks (PB 1–3). Twelve or more replicates per concentration (n ≥ 12). PPARγ = peroxisome proliferator receptor gamma, GR = glucocorticoid receptor, LOD = limit of detection.

Fig. S23. Dose-response relationships for (A) PPARγ and (B) GR activity of the reference compound rosiglitazone and dexamethasone. 48 or more replicates per concentration (n ≥ 48). PPARγ = peroxisome proliferator receptor gamma, GR = glucocorticoid receptor, LOD = limit of detection, VC = vehicle control.

Fig. S24. Dose-response relationship for the reference compound rosiglitazone in the adipogenesis assay without dexamethasone in the differentiation medium. (A) proliferation normalized on the mean of the vehicle control, (B) lipid droplet count per field, (C) adipocyte count per field, (D) mature adipocyte count per field, (E) total intensity of the NileRed staining within the

lipid droplet mask per field and (F) total area occupied by lipid droplets per field. Eight or more replicates per concentration (n ≥ 8). VC = vehicle control, RFU = relative fluorescence unit.

Table S1. Cell viability (%) of the cytotoxic samples in the reporter gene assay experiments. PPARγ = peroxisome proliferator receptor gamma, GR = glucocorticoid receptor, SD = standard deviation.

Table S2. The chemicals tentatively identified using GC-QTOF-MS/MS (data from Zimmermann *et al.* (13)).

Table S3. List of adipogenic chemicals based on the published literature.

Table S4. Comparison of the adipogenic effects of plastic extracts and the abundance of three metabolic disrupting chemicals detected in at least three samples, diphenyl phosphate (DPP), 2-ethylhexyl diphenyl phosphate (EHDP), and triphenyl phosphate (TPP) in the LC-QTOF-MS/MS.